AIAA JOURNAL
Vol. 33, No. 4, April 1995

Force and Moment on a Joukowski Profile in the Presence of Point Vortices

K. Streitlien* and M. S. Triantafyllou†
Massachusetts Institute of Technology, Cambridge, Massachusetts 02139-4307

We present closed-form expressions for the force and moment on a Joukowski profile in arbitrary motion, surrounded by point vortices that are free to convect with the local flow. Thus, rapid and accurate calculation of force and moment in ideal flow simulations is facilitated.

I. Introduction

FOR many purposes, inviscid flow simulation by means of two-dimensional potential flow theory and point vortices provides valuable information about unsteady flow over high-aspect-ratio wings.[1,2] One way of calculating the flowfield and vortex convection velocities is to represent the foil shape as a conformal mapping of a circle, making use of the powerful theory of functions of a complex variable.[3–5] The wake of the profile is discretized into point vortices, and the circle theorem insures that the body boundary condition is satisfied everywhere on the foil. Assuming that the Kutta condition of finite flow velocity at the trailing edge holds,[6] new vortices of the appropriate strength are continually released in the wake. An algorithm for time integration is all that is needed to complete the simulation of large-amplitude foil motion. In cases where the exact profile shape is of secondary importance, a Joukowski mapping can be used, and the resulting expressions for the complex potential become particularly simple.[7–11]

We show that the force and moment acting on the Joukowski profile throughout the simulation consist of added mass terms as if the flow were free of vortices plus the summed effect of all of the vortices in the flow.

II. Flow Description

In Fig. 1, the circle C in the ζ plane is transformed to a Joukowski foil S in the physical plane, $z = x + iy$, by

$$z = F(\zeta) = \zeta + \zeta_c + \frac{a^2}{\zeta + \zeta_c} \tag{1}$$

where a and ζ_c are parameters that determine the size, thickness, and camber of the foil, and C has radius $r_c = |a - \zeta_c|$. Three quantities of interest are the area A, moment of area $z_c A$, and polar moment of area $r_g^2 A$ for the Joukowski foil. These can be found using a complex form of Stokes' theorem[12]:

$$A = \pi r_c^2 \left[1 - \frac{a^4}{\left(r_c^2 - \delta^2\right)^2} \right] \tag{2}$$

$$z_c A = \pi r_c^2 \left[\zeta_c + \frac{a^6 \bar{\zeta}_c}{\left(r_c^2 - \delta^2\right)^3} \right] \tag{3}$$

$$r_g^2 A = \frac{\pi}{2} r_c^2 \left[r_c^2 + 2\delta^2 - a^8 \frac{r_c^2 + 2\delta^2}{\left(r_c^2 - \delta^2\right)^4} \right] \tag{4}$$

where $\delta = |\zeta_c|$.

The z coordinate system is presumed to be at rest in the fluid at infinity, coinciding with the foil only at the instant under consideration. In this reference frame, the foil is translating with velocities U and V in the x and y directions, respectively (forward motion corresponding to a negative value of U). Furthermore, the foil rotates counterclockwise about the origin at a rate Ω. The flow in the z plane is described completely by the complex potential:

$$w = U w_1(\zeta) + V w_2(\zeta) + \Omega w_3(\zeta) + \gamma_c w_4(\zeta) + \sum_k \gamma_k w_5(\zeta; \zeta_k) \tag{5}$$

$$w_1 = -\frac{r_c^2}{\zeta} + \zeta_c + \frac{a^2}{\zeta + \zeta_c} \tag{6}$$

$$w_2 = -i\frac{r_c^2}{\zeta} - i\zeta_c - i\frac{a^2}{\zeta + \zeta_c} \tag{7}$$

$$w_3 = -i \left[\frac{\zeta_c r_c^2}{\zeta} + a^2 \frac{r_c^2/\zeta + \bar{\zeta}_c}{\zeta + \zeta_c} + \frac{a^4 \zeta_c}{(\zeta + \zeta_c)\left(r_c^2 + \delta^2\right)} + \frac{a^4 + r_c^4 - \delta^4}{2\left(r_c^2 - \delta^2\right)} \right] \tag{8}$$

$$w_4 = i \log \frac{\zeta}{r_c} \tag{9}$$

$$w_5 = i \log \left(-\frac{r_c}{\zeta_k} \frac{\zeta - \zeta_k}{\zeta - r_c^2/\bar{\zeta}_k} \right) \tag{10}$$

and the mapping $z = F(\zeta)$, where w_1, w_2, and w_3 are unit velocity potentials for surge, heave, and pitch, respectively; w_4 is the unit potential for a central vortex at $\zeta = 0$; and w_5 is the unit potential for a free vortex at $z_k = F(\zeta_k)$. Overbars denote a complex conjugate. The free vortex potential consists of the vortex itself and its oppositely signed image at the inverse point in accordance with the circle theorem.[12] The two vortex potentials are in a form such that

$$\operatorname{Im} w_4 = \operatorname{Im} w_5 = 0, \quad \text{on } S \tag{11}$$

and

$$w_5 \to -w_4, \quad \text{as } \zeta_k \to \infty \tag{12}$$

It can be verified that this flow satisfies the body boundary condition,[13]

$$\psi = \operatorname{Im} w = Uy - Vx - \tfrac{1}{2}\Omega z\bar{z}, \quad \text{on } S \tag{13}$$

behaves properly at infinity,

$$\frac{\mathrm{d}w}{\mathrm{d}z} \to 0, \quad \text{as } z \to \infty \tag{14}$$

Received Feb. 5, 1994; revision received July 29, 1994; accepted for publication Oct. 3, 1994.

*Graduate Research Assistant, Department of Ocean Engineering; currently Postdoctoral Research Associate, Levich Institute, Mechanical Engineering Department, City College of New York, New York, NY 10031.

†Professor, Department of Ocean Engineering.

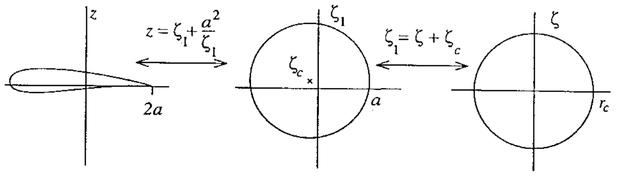

Fig. 1 Mapping between Joukowski profile and circle.

is analytic everywhere in the flow, except at the trailing edge and at vortex locations, $z_k = F(\zeta_k)$, and has the correct singular behavior at the vortex locations,

$$w \sim i\gamma_k \log(z - z_k), \quad \text{as } z \to z_k \tag{15}$$

A full account of the derivation of w, as well as the calculations that follow, can be found in Ref. 14.

Note that the strength of the vortices differs from what other researchers use by a factor of -2π. Thus, the total counterclockwise circulation about the foil caused by the free vortex images and the central vortex is

$$\Gamma = 2\pi\left(\sum_k \gamma_k - \gamma_c\right) \tag{16}$$

The vortices convect with velocities given by Routh's rule[9,15,16]:

$$\begin{aligned}\frac{\mathrm{d}\bar{z}_k}{\mathrm{d}t} &= \frac{\mathrm{d}}{\mathrm{d}z}[w(z) - i\gamma_k \log(z - z_k)]_{z=z_k} \\ &= \left\{\frac{\mathrm{d}}{\mathrm{d}\zeta}[w - i\gamma_k \log(\zeta - \zeta_k)]\frac{1}{\mathrm{d}F/\mathrm{d}\zeta}\right\}_{\zeta=\zeta_k} \\ &\quad - \frac{i\gamma_k}{2}\left[\frac{\mathrm{d}^2F/\mathrm{d}\zeta^2}{[\mathrm{d}F/\mathrm{d}\zeta]^2}\right]_{\zeta=\zeta_k}\end{aligned} \tag{17}$$

Closed-form expressions are obtained upon substitution of Eqs. (1) and (5–10).

There is no unique way to perform simulations of nonlinear foil motion based on Eq. (17), and the force and moment expressions that follow are not restricted to a particular simulation procedure. However, to put the present work in a practical context and make the results reproducible, we will briefly describe our own simulation algorithm.

A Joukowski foil executes a prescribed motion, from which velocities and accelerations can be obtained at any desired time.

Vortices are released at the trailing edge according to the following algorithm: At the beginning of a time step, we form a circular arc tangent to the trailing edge and passing through z_{N-1}, the location of the previously shed vortex. We place the new vortex at a point on this arc, z_N, such that the distance from the trailing edge to z_N is $\frac{1}{4}$ of the distance to z_{N-1}, both measured along the arc. By this method the vortices are introduced in the middle of the appropriate segment of a continuous vortex sheet that we try to represent. The strength of the new vortex is determined such that the point on the circle C that maps onto the trailing edge is a stagnation point in the ζ plane. This is the classical Kutta condition that insures smooth flow over the trailing edge at the beginning of every time step. The position for the very first vortex must be chosen somewhere in the neighborhood of the trailing edge, but this choice is not critical. This vortex-shedding scheme is easy to implement, contains no disposable parameters or iteration procedures, and has proven robust for arbitrary large angles of attack. Of course, it is only applicable to foil shapes with a cusped trailing edge.

A second-order Runge–Kutta integration scheme is used to step the solution forward in time. The $\mathcal{O}(N^2)$ (N being the number of vortices) computational effort required by direct evaluation of Eq. (17) can be reduced by a method based on multipole expansions of the vortex interactions.[17,18] Our colleague F. T. Korsmeyer kindly provided an influence algorithm that employs the multipole expansion method,[19] which reduces the operation count to $\mathcal{O}(N)$ for large N. The algorithm was adapted to treat the image vortices within the circle C efficiently.

At every time step, vortex positions and velocities are stored for postprocess force and moment calculation.

III. Force

Representing the forces per unit span X and Y along the x and y axes as one complex number, Milne-Thomson[12] gives

$$\begin{aligned}X + iY = {}& -i\frac{\mathrm{d}}{\mathrm{d}t}\int_S w\,\mathrm{d}z + \dot{W}A + i\dot{\Omega}Az_c - \overline{\frac{i}{2}\int_S\left(\frac{\mathrm{d}w}{\mathrm{d}z}\right)^2\mathrm{d}z} \\ & - \Omega\int_S z\,\mathrm{d}w + iW\Gamma + i\Omega A(W + i\Omega z_c)\end{aligned} \tag{18}$$

where the dot indicates time derivative. The velocity has been written as a complex number, $W = U + iV$, and unit fluid density is assumed. This expression is obtained by integrating the pressure in a coordinate system that is fixed in the foil, z', for example. In this reference frame, S is independent of time, and consequently the time derivative could be taken outside the integral sign.

The three integrals in Eq. (18) can be evaluated by forming the integration contour shown in Fig. 2, where only one free vortex is considered. The term S_b encloses the branch cut between the vortex and its image, passing through the trailing edge z_t, S_v surrounds the vortex at an arbitrarily small radius, and S_∞ closes the contour at a large distance. The location of the vortex is denoted z'_k as a reminder that its time derivative must be taken as seen by an observer moving with the foil at all times. This is important because the two coordinate systems are moving relative to each other but coincide at the instant in question; thus,

$$z'_k = z_k = F(\zeta_k) \tag{19}$$

but

$$\frac{\mathrm{d}z'_k}{\mathrm{d}t} = \frac{\mathrm{d}z_k}{\mathrm{d}t} - W - i\Omega z_k = \frac{\mathrm{d}}{\mathrm{d}t}F(\zeta_k) \tag{20}$$

The integrands in Eq. (18) are analytic in the region enclosed by the entire contour; consequently,

$$\int_S = \int_{S_\infty} - \int_{S_v} - \int_{S_b} \tag{21}$$

Integrals over S can therefore be replaced by others that are easier to evaluate. We will take all integrals to be in the counterclockwise direction.

This method has been used by Sarpkaya[7] and Graham[20] for flow over stationary objects. It is an extension of Lagally's theorem, which is valid for steady flow.

In cases where the foil starts to move from an initial state of rest and the fluid is otherwise undisturbed, the total circulation around the foil and its wake must remain zero by virtue of Kelvin's circulation theorem. This implies that $\gamma_c = 0$ at all times. In the general case, vortices other than those shed at the trailing edge may be introduced in the flow at any time. Then, γ_c must change so as to preserve the circulation around the foil alone. When $\gamma_c = 0$, it is possible to evaluate the integrals in Eq. (18) for arbitrary profile shapes except

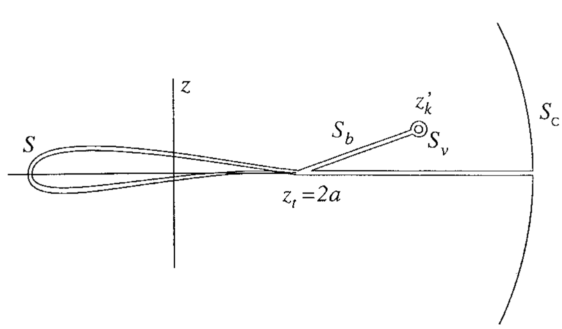

Fig. 2 Integration contour for force.

for the contributions from S_∞. Deferring the details to Appendix A, we obtain

$$\int_S w\,\mathrm{d}z = \int_{S_\infty} w\,\mathrm{d}z - 2\pi\gamma_k(z_k' - z_t) \tag{22}$$

$$\overline{\int_S \left(\frac{\mathrm{d}w}{\mathrm{d}z}\right)^2 \mathrm{d}z} = 4\pi\gamma_k\left(\frac{\mathrm{d}z_k'}{\mathrm{d}t} + W + i\Omega z_k'\right) \tag{23}$$

$$\int_S z\,\mathrm{d}w = \int_{S_\infty} \frac{\mathrm{d}w}{\mathrm{d}z} z\,\mathrm{d}z + 2\pi\gamma_k z_k' \tag{24}$$

The result is a general force expression that requires only the far-field behavior of w:

$$\begin{aligned} X + iY = {} & -i\frac{\mathrm{d}}{\mathrm{d}t}\left[\int_{S_\infty} w\,\mathrm{d}z - 2\pi\sum_k \gamma_k(z_k' - z_t)\right] \\ & + \dot{W}A + i\dot{\Omega}Az_c - 2\pi i\sum_k \gamma_k\frac{\mathrm{d}z_k'}{\mathrm{d}t} \\ & - \int_{S_\infty} \frac{\mathrm{d}w}{\mathrm{d}z} z\,\mathrm{d}z + i\Omega A(W + i\Omega z_c) \end{aligned} \tag{25}$$

The vortex terms being linear, we extended the result to an arbitrary number of vortices simply by summing the individual contributions. If the number of vortices around the profile remains constant, the time derivative may be taken inside the first summation, and cancellation with the second sum is obtained. When vortices are continually released in the flow, however, the time derivative should be left outside the sum to account for the changing number of vortices.

In the case of a Joukowski foil with arbitrary γ_c, Eqs. (5–10) can be substituted for w, and we find

$$\begin{aligned} \int_S w\mathrm{d}z = 2\pi\Big[& iU\left(a^2 - r_c^2\right) + V\left(a^2 + r_c^2\right) \\ & + \Omega\left(r_c^2\zeta_c + a^2\bar{\zeta}_c - \frac{a^4\zeta_c}{r_c^2 - \delta^2}\right) + \gamma_c(2a - \zeta_c) \\ & + \gamma_k\left(\zeta_k - r_c^2/\bar{\zeta}_k - z_k' + 2a\right)\Big] \end{aligned} \tag{26}$$

$$\begin{aligned} \int_S z\,\mathrm{d}w = 2\pi\Big[& iU\left(r_c^2 - a^2\right) - V\left(r_c^2 + a^2\right) \\ & - \Omega\left(r_c^2\zeta_c + a^2\bar{\zeta}_c - \frac{a^4\zeta_c}{r_c^2 - \delta^2}\right) \\ & + \gamma_c\zeta_c + \gamma_k\left(\frac{r_c^2}{\bar{\zeta}_k} - \zeta_k + z_k'\right)\Big] \end{aligned} \tag{27}$$

With these results, plus Eq. (2) and Eq. (3), substituted into Eq. (18), an explicit force formula is obtained. The conventional added mass notation[21] and the relations of Eqs. (16) and (20) provide a compact expression:

$$\begin{aligned} X + iY = {} & -\dot{U}(m_{11} + im_{21}) - \dot{V}(m_{12} + im_{22}) \\ & - \dot{\Omega}(m_{16} + im_{26}) + \Omega U(m_{21} - im_{11}) \\ & + \Omega V(m_{22} - im_{12}) + \Omega^2(m_{26} - im_{16}) \\ & + i(W + i\Omega\zeta_c)\Gamma + i\frac{\mathrm{d}}{\mathrm{d}t}[2\pi\mathcal{Z}_1 - \Gamma(2a - \zeta_c)] \\ & - 2\pi i\mathcal{Z}_2 - 2\pi\Omega\mathcal{Z}_1 \end{aligned} \tag{28}$$

where

$$m_{11} = \pi r_c^2 - 2\pi a^2 + \pi r_c^2\frac{a^4}{\left(r_c^2 - \delta^2\right)^2} \tag{29}$$

$$m_{12} = 0 \tag{30}$$

$$m_{21} = 0 \tag{31}$$

$$m_{22} = \pi r_c^2 + 2\pi a^2 + \pi r_c^2\frac{a^4}{\left(r_c^2 - \delta^2\right)^2} \tag{32}$$

$$m_{16} = \mathrm{Im}\left[-\pi r_c^2\zeta_c - 2\pi a^2\bar{\zeta}_c + 2\pi\frac{a^4\zeta_c}{r_c^2 - \delta^2} + \pi r_c^2\frac{a^6\bar{\zeta}_c}{\left(r_c^2 - \delta^2\right)^3}\right] \tag{33}$$

$$m_{26} = \mathrm{Re}\left[\pi r_c^2\zeta_c + 2\pi a^2\bar{\zeta}_c - 2\pi\frac{a^4\zeta_c}{r_c^2 - \delta^2} - \pi r_c^2\frac{a^6\bar{\zeta}_c}{\left(r_c^2 - \delta^2\right)^3}\right] \tag{34}$$

$$\mathcal{Z}_1 = \sum_k \gamma_k\left(\frac{r_c^2}{\bar{\zeta}_k} + \frac{a^2}{\zeta_k + \zeta_c}\right) \tag{35}$$

$$\mathcal{Z}_2 = \sum_k \gamma_k\frac{\mathrm{d}z_k}{\mathrm{d}t} \tag{36}$$

The added mass coefficients m_{ij} have been verified against Sedov's expressions.[22]

The terms $\mathcal{Z}_i$ are sums involving all of the free vortices. The vortex convection velocities in $\mathcal{Z}_2$, given by Eq. (17), are expensive to calculate. However, these velocities are needed to perform the simulation, and so there is no extra effort required for the force calculation.

IV. Moment

Milne-Thomson[12] gives the counterclockwise moment about $z = 0$:

$$\begin{aligned} M = \mathrm{Re}\Big[& -\frac{\mathrm{d}}{\mathrm{d}t}\int_S wz\,\mathrm{d}\bar{z} - 3i\dot{\bar{W}}z_cA - 2\dot{\Omega}r_g^2A \\ & - \frac{1}{2}\int_S\left(\frac{\mathrm{d}w}{\mathrm{d}z}\right)^2 z\,\mathrm{d}z + \bar{W}\int_S z\,\mathrm{d}w + \Omega\bar{W}z_cA\Big] \end{aligned} \tag{37}$$

Note that additive constants in w will give a contribution to the first integral, and so it is important to formulate all of the potentials w_i so that the boundary condition of Eq. (13) holds without added constants.

The first integrand is not analytic, and the contour decomposition that we used in the force calculation is not applicable here. Thus, no general expression equivalent to Eq. (25) exists. Instead, the mapping function $F(\zeta)$ will be substituted for z and the integral evaluated on the map circle C, where we may use the fact that $\bar{\zeta} = r_c^2/\zeta$ to render the integrand analytic. By virtue of Eq. (5), the first integral can be broken down into smaller ones:

$$\begin{aligned} \int_S wz\,\mathrm{d}\bar{z} = {} & U\int_S w_1z\,\mathrm{d}\bar{z} + V\int_S w_2z\,\mathrm{d}\bar{z} + \Omega\int_S w_3z\,\mathrm{d}\bar{z} \\ & + \gamma_c\int_S w_4z\,\mathrm{d}\bar{z} + \sum_k\gamma_k\int_S w_5z\,\mathrm{d}\bar{z} \end{aligned} \tag{38}$$

The details of their evaluation are given in Appendix B; these are the final results:

$$\begin{aligned} \int_S w_1z\,\mathrm{d}\bar{z} = 2\pi i\Bigg\{ & -a^2\zeta_c + a^4\bar{\zeta}_c\left[\frac{1}{r_c^2 - \delta^2} + \frac{r_c^2}{\left(r_c^2 - \delta^2\right)^2}\right] \\ & - 2\frac{a^6r_c^2}{\left(r_c^2 - \delta^2\right)^3}\bar{\zeta}_c - r_c^2\zeta_c + \frac{a^4r_c^2}{\left(r_c^2 - \delta^2\right)^2}\zeta_c\Bigg\} \end{aligned} \tag{39}$$

$$\int_S w_2 z\, \mathrm{d}\bar{z} = 2\pi \left\{ a^2\zeta_c - a^4\bar{\zeta}_c \left[\frac{1}{r_c^2-\delta^2} + \frac{r_c^2}{\left(r_c^2-\delta^2\right)^2} \right] \right.$$
$$\left. - 2\frac{a^6 r_c^2}{\left(r_c^2-\delta^2\right)^3}\bar{\zeta}_c - r_c^2\zeta_c + \frac{a^4 r_c^2}{\left(r_c^2-\delta^2\right)^2}\zeta_c \right\} \tag{40}$$

$$\int_S w_3 z\, \mathrm{d}\bar{z} = 2\pi \left[a^4 + a^2\zeta_c^2 + a^4\frac{\delta^4 - 2r_c^2\delta^2}{\left(r_c^2-\delta^2\right)^2} \right.$$
$$+ \frac{a^6\bar{\zeta}_c^2}{\left(r_c^2-\delta^2\right)^2} + \frac{2a^8 r_c^2\delta^2}{\left(r_c^2-\delta^2\right)^4} - r_c^2\frac{a^4 + r_c^4 - \delta^4}{2\left(r_c^2-\delta^2\right)}$$
$$\left. + a^4 r_c^2 \frac{a^4 + r_c^4 - \delta^4}{\left(r_c^2-\delta^2\right)^3} \right] \tag{41}$$

$$\mathrm{Re}\int_S w_4 z\, \mathrm{d}\bar{z} = -2\pi\,\mathrm{Re}\left(a^2 - \delta^2 + a\zeta_c + \frac{a^3\zeta_c}{\delta^2 - r_c^2} \right) \tag{42}$$

$$\mathrm{Re}\int_S w_5 z\, \mathrm{d}\bar{z} = 2\pi\,\mathrm{Re}\left[\frac{-r_c^2\zeta_c}{\zeta_k} - \frac{a^2 r_c^2}{\zeta_k(\zeta_k+\zeta_c)} + a^2 - \delta^2 \right.$$
$$\left. - \frac{a^4\zeta_c}{\left(\delta^2 - r_c^2\right)(\zeta_k+\zeta_c)} - \frac{a^2\bar{\zeta}_c}{\zeta_k+\zeta_c} + a\zeta_c + \frac{a^3\zeta_c}{\delta^2 - r_c^2} \right] \tag{43}$$

By the same method used for Eq. (37), we find

$$\int_S \left(\frac{\mathrm{d}w}{\mathrm{d}z}\right)^2 z\, \mathrm{d}z = 4\pi\gamma_k \frac{\mathrm{d}\bar{z}_k}{\mathrm{d}t} z_k \tag{44}$$

Finally, the last integral in Eq. (23) is the same as that in Eq. (27).

Collecting all of these results, one can write the moment in the following compact form:

$$M = -\dot{U}m_{61} - \dot{V}m_{62} - \dot{\Omega}m_{66} - U^2 m_{21} + V^2 m_{12}$$
$$+ UV(m_{11} - m_{22}) - U\Omega m_{26} + V\Omega m_{16}$$
$$+ \frac{\mathrm{d}}{\mathrm{d}t}\left[2\pi\mathcal{S}_1 - \Gamma\,\mathrm{Re}\left(a^2 - \delta^2 + a\zeta_c + \frac{a^3\zeta_c}{\delta^2 - r_c^2} \right) \right]$$
$$- 2\pi\mathcal{S}_2 + \mathrm{Re}[\bar{W}(2\pi\mathcal{Z}_3 - \Gamma\zeta_c)] \tag{45}$$

where

$$m_{61} = m_{16} \tag{46}$$

$$m_{62} = m_{26} \tag{47}$$

$$m_{66} = 2\pi\,\mathrm{Re}\left[a^4 + a^2\zeta_c^2 + a^4\frac{\delta^4 - 2r_c^2\delta^2}{\left(r_c^2-\delta^2\right)^2} + \frac{a^6\bar{\zeta}_c^2}{\left(r_c^2-\delta^2\right)^2} \right.$$
$$\left. + \frac{2a^8 r_c^2\delta^2}{\left(r_c^2-\delta^2\right)^4} - r_c^2\frac{a^4 + r_c^4 - \delta^4}{2(r_c^2 - \delta^2)} + a^4 r_c^2\frac{a^4 + r_c^4 - \delta^4}{\left(r_c^2-\delta^2\right)^3} \right] \tag{48}$$

$$\mathcal{S}_1 = \sum_k \gamma_k \mathrm{Re}\left[\frac{r_c^2\zeta_c}{\zeta_k} + \frac{a^2 r_c^2}{\zeta_k(\zeta_k+\zeta_c)} \right.$$
$$\left. + \frac{a^4\zeta_c}{\left(\delta^2 - r_c^2\right)(\zeta_k+\zeta_c)} + \frac{a^2\bar{\zeta}_c}{\zeta_k+\zeta_c} \right] \tag{49}$$

$$\mathcal{S}_2 = \sum_k \gamma_k \mathrm{Re}\left(\frac{\mathrm{d}\bar{z}_k}{\mathrm{d}t} z_k \right) \tag{50}$$

$$\mathcal{Z}_3 = \sum_k \gamma_k \left(\frac{r_c^2}{\bar{\zeta}_k} + \frac{a^2}{\zeta_k + \zeta_c} \right) \tag{51}$$

V. Examples

In this section we provide a number of example calculations to compare against previous results and demonstrate the use of the derived expressions. The time derivatives of the expressions in square brackets in (28) and (45) are evaluated using central differences, which yield the time derivative at the middle of each time step. The values of Γ, $\mathcal{S}_2$, $\mathcal{Z}_1$, $\mathcal{Z}_2$, and $\mathcal{Z}_3$ are interpolated to the middle of each time step. The added mass forces are exactly computed at these intermediate times.

A. Impulsively Started Flat Plate at Small Angle of Attack

In the first example, we compare our expressions with linear theory for an impulsively started flat plate at small angle of attack.

The input parameters for this and the following two examples are listed in Table 1.

Figure 3 shows how the numerically predicted forces converge to the theoretical results as the time step is reduced, except at $t = 0$. Lift, drag, and clockwise moment have been normalized with $2\pi U^2 c\alpha_0$, $U^2 c\alpha_0^2$, and $\pi U^2 c^2\alpha_0$, respectively. Since there are no added mass forces in this case, the example shows clearly how well the effect of the vortex wake is modeled. An analysis of the pressure distribution reveals that the deviation from linear theory is confined to the region near the trailing edge. The wake of the foil, consisting of discrete vortices, cannot reproduce the velocity discontinuity at the trailing edge, which is necessary for zero loading at this point. As we decrease the time step, the region of this discrepancy shrinks for finite times, but the amplitude of the trailing-edge loading does not. The theory also shows that the velocity jump is proportional to $\mathrm{d}\Gamma/\mathrm{d}t$, which has a $t^{-\frac{1}{2}}$ singularity, here explaining the nonuniform behavior at $t = 0$.

B. Impulsively Started Thick Foil at Small Angle of Attack

Figure 4 shows that the lift force on a foil with finite thickness, normalized by its steady-state value, builds up slower than for a flat plate. The results compare well with those of Giesing[2] and with the theoretical value at $t = 0$ found by the method of Chow and Huang.[23]

C. Impulsively Started Foil at Large Angle of Attack

Figure 5 shows the normalized lift response at a very large angle of attack. In this case the finite loading at the trailing edge produces an incorrect initial force, but after a nondimensional time of about 0.5, the response agrees well with Giesing's results, although he used a von Mises profile shape.

D. Large-Amplitude Foil Oscillation

Next, a symmetric foil executing large-amplitude heave and pitch in a uniform inflow is simulated with the parameters given in Table 2. This is the model of a flapping foil used as a propulsive device. The motion of the foil is described in a reference frame at the mean position of the foil. The velocities are transformed to the z coordinate system, to give U and V in the force expressions, as well as the time derivatives. The forces to the original reference frame. As the force and moment records in Fig. 6 show, this case is well beyond the scope of linear theory, from which sinusoidally varying forces would be predicted. However, we notice that a periodic time dependence is established in very short time, indicating that the added mass forces dominate in this case. For foils with a rounded leading edge, we can also evaluate the integrals in Eqs. (18) and (37) numerically as a check.

Table 1 Input parameters for impulsively started foil

Example	5.1	5.2	5.3
a	0.5	0.5	0.5
ζ_c	0	−0.124	−0.035
Chord length $2c$	2	2.01	2.08
Thickness, %	0	25.5	8.4
Freestream velocity U	1.0	1.0	1.0
Pitch angle, rad	0.01	0.01	0.8
Time step	0.025–0.4	0.05	0.04

Table 2 Input parameters for oscillating foil

a	0.5
ζ_c	−0.05
Chord length $2c$	2.02
Thickness, %	12
Free stream velocity U	1.0
Heave amplitude h_0	0.9
Pitch amplitude α_0, rad	0.6
Pitch point b	0.0
Oscillation period, $T = 2\pi/\omega$	3.0
Reduced frequency, $\omega c/U$	2.1
Time step	0.04

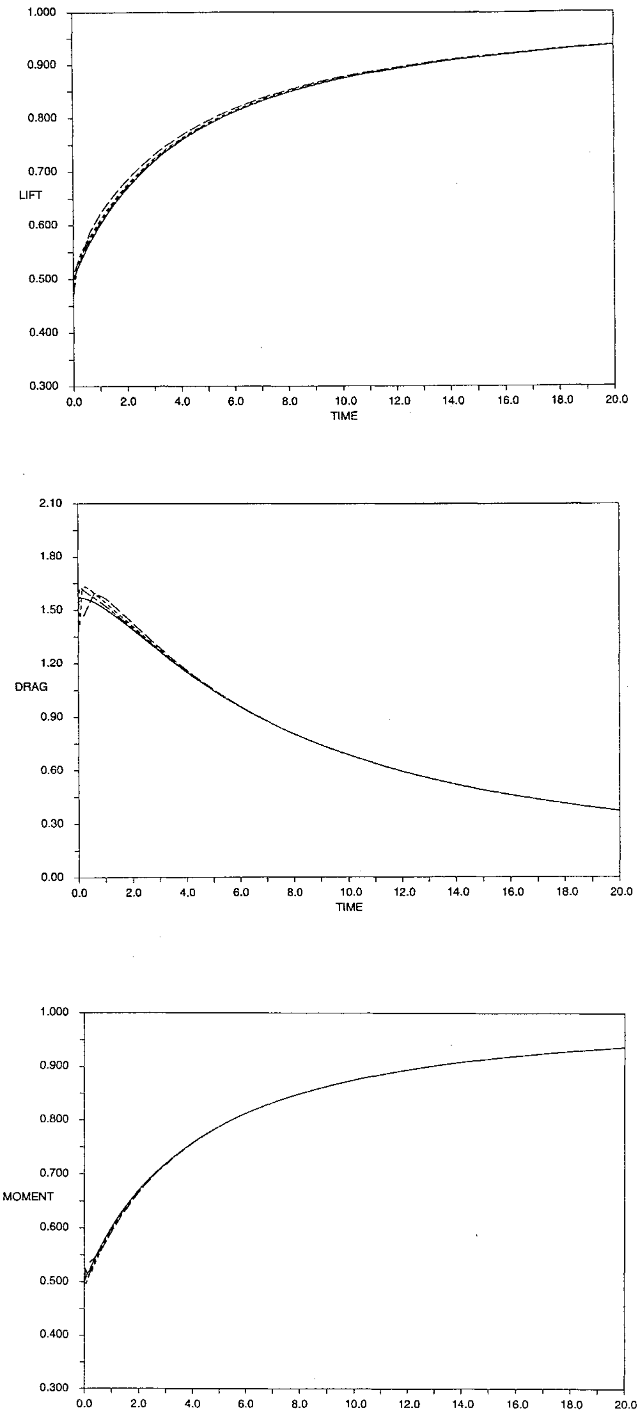

Fig. 3 Forces on an impulsively started flat plate at small angle of attack: ——, linear theory; — — —, time step = 0.4; - - - - -, time step = 0.1; and - · - · -, time step = 0.025.

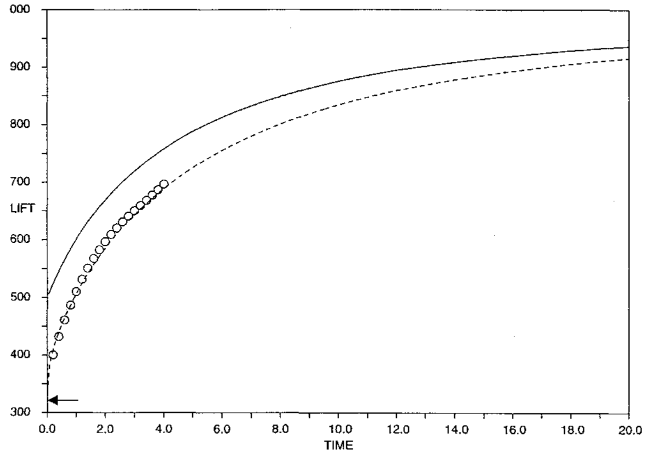

Fig. 4 Forces on an impulsively started 25% thick Joukowski foil at small angle of attack: ——, linear theory; - - - - -, present results; οο, Giesing; and Δ, Chow and Huang.

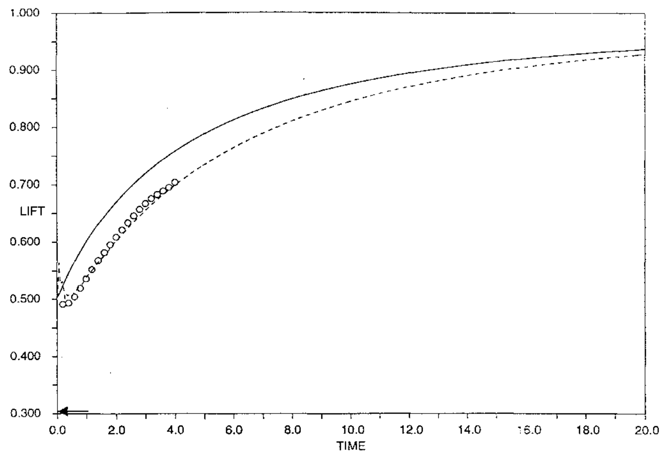

Fig. 5 Forces on an impulsively started 8.4% thick Joukowski foil at large angle of attack (0.8 rad): ——, linear theory; - - - - -, present results; οο, Giesing; and Δ, Chow and Huang.

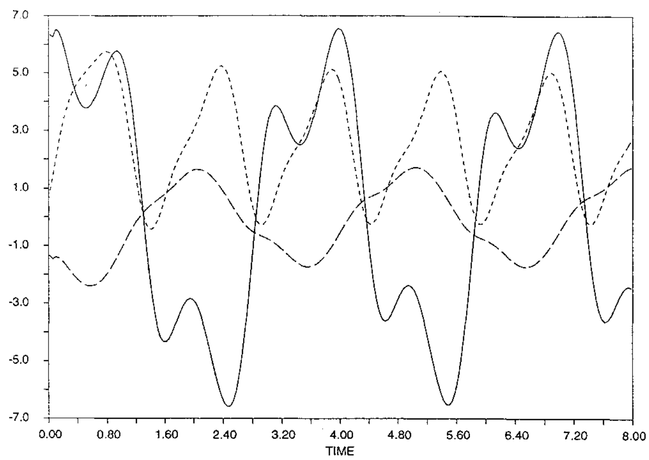

Fig. 6 Forces on a symmetric foil in large-amplitude oscillation: ——, lift; — — —, moment; and - - - - -, thrust.

The results agree with the closed-form expressions to whatever precision we can evaluate the integrals. The biggest difference in the response is due to the fact that time derivatives of velocities are in effect obtained from numerical differentiation when the integrals are evaluated numerically. Numerical integration is difficult to do when the foil has zero thickness and takes much longer to perform than using Eqs. (28) and (45). For 10^{-4} accuracy, for instance, it takes about 40 times longer to integrate Eqs. (18) and (37) with NAG routines d01ajf and d01aqf, than it takes to evaluate Eqs. (28) and (45).

Table 3 Input parameters for vortex passing over a stationary foil

a	0.5
ζ_c	$-0.05 + i0.05$
Chord length $2c$	2.02
Thickness, %	12
Freestream velocity U	1.0
Time step	0.08
Upstream vortex strength	0.5
Upstream vortex release point	$-6 + i0.5$

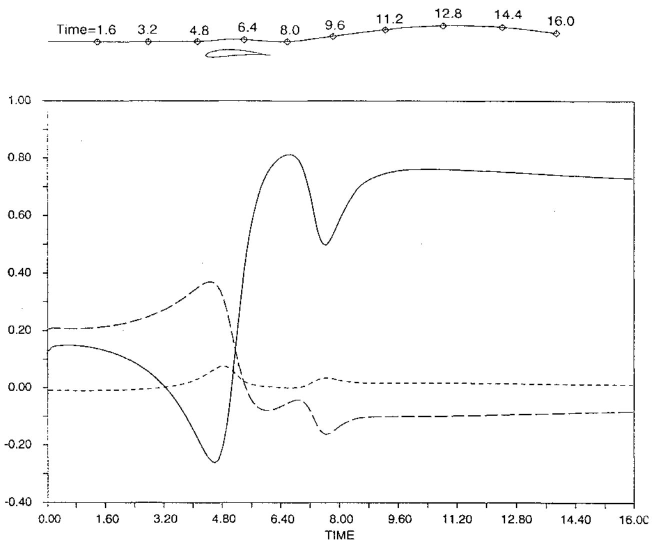

Fig. 7 Blade-vortex interaction: ——, lift; — — —, moment; and - - - - -, thrust.

E. Vortex Passing over a Cambered Foil

The last example is a case of blade-vortex interaction with the parameters given in Table 3. A discrete vortex is released at a point upstream of a stationary, cambered foil, convecting with the freestream. The path of the vortex, shown in Fig. 7, is first affected by the presence of the foil and the image vortex inside it. Then downstream of the foil, the vorticity shed at the trailing edge due to the downwash on the foil causes the vortex to migrate away from the x axis. The force record shows that maximum lift on the foil occurs as the vortex passes over the trailing edge.

VI. Comments

By evaluating the integrals in the general expressions provided by Milne-Thomson,[12] we have obtained formulas for force and moment experienced by a Joukowski foil in a flow with point vortices. The principal differences from previous work can be summarized as follows:

1) No integrations over the foil surface are necessary.

2) The profile shape is a general Joukowski foil, compared with a flat plate in Refs. 7 and 24 and a general power series transform in Ref. 20. On the other hand, the force expression in Ref. 24 is more general with respect to the description of the wake.

3) The profile is allowed to perform arbitrary motion in a fluid at rest. This is more general than flow over a stationary profile[7,20] which is kinematically equivalent in the case of translation but precludes treatment of rotation.

4) To the authors' knowledge, no closed-form expression has been published for the moment, even in the special case of a flat plate.

Appendix A: Integrals for Force Expression

In the first integral of Eq. (18) we note that the logarithmic singularity at z_k is too weak to give a contribution as S_v shrinks. Furthermore, $\int w_4\,\mathrm{d}z$ is not suited to evaluation on the contour in Fig. 2 and will be evaluated later directly on S. Omitting w_4, the first integral gets a contribution from the cut S_b, where w makes a jump $2\pi\gamma_k$ from the upper to the lower bank and from S_∞. Thus we get Eq. (22).

Limiting ourselves to the previously defined Joukowski profile, we can readily find the far-field behavior of w and identify the terms that go like $1/z$. By the residue theorem we then find the contribution from S_∞:

$$\int_{S_\infty} w\,\mathrm{d}z = 2\pi\Bigg[iU\left(a^2 - r_c^2\right) + V\left(a^2 + r_c^2\right) + \Omega\left(r_c^2\zeta_c + a^2\bar{\zeta}_c - \frac{a^4\zeta_c}{r_c^2 - \delta^2}\right) + \gamma_k\left(\zeta_k - \frac{r_c^2}{\bar{\zeta}_k}\right)\Bigg] \tag{A1}$$

Then we must add the contribution from $\gamma_c w_4$ by integrating by parts on S:

$$\int_S w_4\,\mathrm{d}z = (w_4 z)_-^+ - \int_S \frac{\mathrm{d}w_4}{\mathrm{d}z} z\,\mathrm{d}z = 2\pi z_{\mathrm{cut}} - \int_C F(\zeta)\,\mathrm{d}w_4 = 2\pi(z_{\mathrm{cut}} - \zeta_c) \tag{A2}$$

The square brackets with limits mean that the difference should be taken at opposite sides of the branch cut associated with the logarithmic potential. Therefore, the value of the integral depends on where this branch cut is chosen to be. We use the property of Eq. (12) to argue that

$$\int_S w_4\,\mathrm{d}z = -\lim_{\zeta_k\to\infty}\int_S w_5\,\mathrm{d}z \tag{A3}$$

implying that the previous z_{cut} is $2a$, i.e., the branch cut for w_4 must pass through the trailing edge as is the case with the free vortices. This results in the expression Eq. (26).

The second integral of Eq. (18) gets no contributions from the cut S_b because the integrand is continuous here. Neither is there a contribution from S_∞, as $w = \mathcal{O}(\log z)$ here. The only contribution is from S_v, and this term is evaluated by separating out the singularity at z_k:

$$w(z) = f_k(z) + i\gamma_k \log(z - z_k) \tag{A4}$$

where $f_k(z)$ is analytic in the neighborhood of z_k,

$$\int_S \left(\frac{\mathrm{d}w}{\mathrm{d}z}\right)^2 \mathrm{d}z = -\int_{S_v}\left[\frac{\mathrm{d}f_k}{\mathrm{d}z} + \frac{i\gamma_k}{z - z_k}\right]^2 \mathrm{d}z = 4\pi\gamma_k\left[\frac{\mathrm{d}f_k}{\mathrm{d}z}\right]_{z=z_k} \tag{A5}$$

From Eq. (17) it is seen that $\overline{[\mathrm{d}f_k/\mathrm{d}z]_{z=z_k}}$ is the convection velocity of the vortex, as seen in the z reference frame; thus,

$$\overline{\int_S \left(\frac{\mathrm{d}w}{\mathrm{d}z}\right)^2 \mathrm{d}z} = 4\pi\gamma_k\frac{\mathrm{d}z_k}{\mathrm{d}t} = 4\pi\gamma_k\left(\frac{\mathrm{d}z_k'}{\mathrm{d}t} + W + i\Omega z_k'\right) \tag{A6}$$

This expression is valid for an arbitrary profile.

In the last integral of Eq. (18), $\gamma_c w_4$ also requires special attention. Apart from this term, we have

$$\int_S z\,\mathrm{d}w = \int_S \frac{\mathrm{d}w}{\mathrm{d}z} z\,\mathrm{d}z \tag{A7}$$

which gets contributions from S_v and S_∞. The former is easily found, leading to

$$\int_S z\,\mathrm{d}w = \int_{S_\infty}\frac{\mathrm{d}w}{\mathrm{d}z} z\,\mathrm{d}z + 2\pi\gamma_k z_k' \tag{A8}$$

For the Joukowski profile, we find terms in $z\,\mathrm{d}w/\mathrm{d}z$ that go like $1/z$ in the far field, and the residue theorem yields

$$\int_{S_\infty} z\,\mathrm{d}w = 2\pi\Bigg[iU\left(r_c^2 - a^2\right) - V\left(r_c^2 + a^2\right) - \Omega\left(r_c^2\zeta_c + a^2\bar{\zeta}_c - \frac{a^4\zeta_c}{r_c^2 - \delta^2}\right) + \gamma_k\left(\frac{r_c^2}{\bar{\zeta}_k} - \zeta_k\right)\Bigg] \tag{A9}$$

We saw previously that

$$\int_S z\,\mathrm{d}w_4 = 2\pi\zeta_c \tag{A10}$$

Collecting terms, we obtain Eq. (27).

Appendix B: Integrals for Moment Expression

For brevity, we shall refer to the integrals in Eq. (38) as I_1 through I_5, respectively;

$$I_1 = \int_C w_1 F(\zeta)\overline{\frac{\mathrm{d}F(\zeta)}{\mathrm{d}\zeta}}\,\mathrm{d}\zeta = \int_C \left(-\frac{r_c^2}{\zeta} + \zeta_c + \frac{a^2}{\zeta+\zeta_c}\right)$$

$$\times\left(\zeta + \zeta_c + \frac{a^2}{\zeta+\zeta_c}\right)\left(1 - \frac{a^2}{\bar\zeta+\bar\zeta_c}\right)\mathrm{d}\bar\zeta$$

$$= \int_C \left(-\frac{r_c^2}{\zeta} + \zeta_c + \frac{a^2}{\zeta+\zeta_c}\right)\left(\zeta+\zeta_c+\frac{a^2}{\zeta+\zeta_c}\right)$$

$$\times\left(-\frac{r_c^2}{\zeta^2} + \frac{a^2 r_c^2}{(r_c^2+\bar\zeta_c\zeta)^2}\right)\mathrm{d}\zeta$$

$$= 2\pi i\left\{-a^2\zeta_c + a^4\bar\zeta_c\left[\frac{1}{r_c^2-\delta^2} + \frac{r_c^2}{\left(r_c^2-\delta^2\right)^2}\right]\right.$$

$$\left. -2\frac{a^6 r_c^2}{\left(r_c^2-\delta^2\right)^3}\bar\zeta_c - r_c^2\zeta_c + \frac{a^4 r_c^2}{\left(r_c^2-\delta^2\right)^2}\zeta_c\right\} \tag{B1}$$

In the second to last step, we used the fact that $\bar\zeta = r_c^2/\zeta$ on C, and in the last step, the integrand was expanded out in 12 terms that were individually evaluated by the residue theorem.

The terms I_2 and I_3 are evaluated similarly; I_4 is difficult to evaluate, and in fact there is no need to do so. Because of Eq. (12), we have

$$I_4 = -\lim_{\zeta_k\to\infty} I_5 \tag{B2}$$

Expanding out, we have

$$I_5 = \int_C i\log\frac{-r_c(\zeta-\zeta_k)}{\zeta_k\left(\zeta - r_c^2/\bar\zeta_k\right)}\left[-\frac{r_c^2}{\zeta} - \frac{r_c^2\zeta_c}{\zeta^2} - \frac{a^2r_c^2}{\zeta^2(\zeta+\zeta_c)}\right.$$

$$\left.+\frac{a^2r_c^2\zeta}{\left(r_c^2+\bar\zeta_c\zeta\right)^2} + \frac{a^2r_c^2\zeta_c}{\left(r_c^2+\bar\zeta_c\zeta\right)^2} + \frac{a^4r_c^2}{(\zeta+\zeta_c)\left(r_c^2+\bar\zeta_c\zeta\right)^2}\right]\mathrm{d}\zeta \tag{B3}$$

Denote the integrand by $g(\zeta)$. A partial fraction expansion of the third and sixth term in the square brackets yields, after collecting terms,

$$g(\zeta) = i\log\frac{-r_c(\zeta-\zeta_k)}{\zeta_k\left(\zeta-r_c^2/\bar\zeta_k\right)}\left[\frac{\mathcal{A}}{\zeta} + \frac{\mathcal{B}}{\zeta^2} + \frac{\mathcal{C}}{\zeta+\zeta_c}\right.$$

$$\left.+\frac{\mathcal{D}}{\zeta+r_c^2/\bar\zeta_c} + \frac{\mathcal{E}+\mathcal{F}\zeta}{\left(\zeta+r_c^2/\bar\zeta_c\right)^2}\right] \tag{B4}$$

where

$$\mathcal{A} = -r_c^2 + r_c^2\frac{a^2}{\zeta_c^2} \tag{B5}$$

$$\mathcal{B} = -r_c^2\zeta_c - r_c^2\frac{a^2}{\zeta_c} \tag{B6}$$

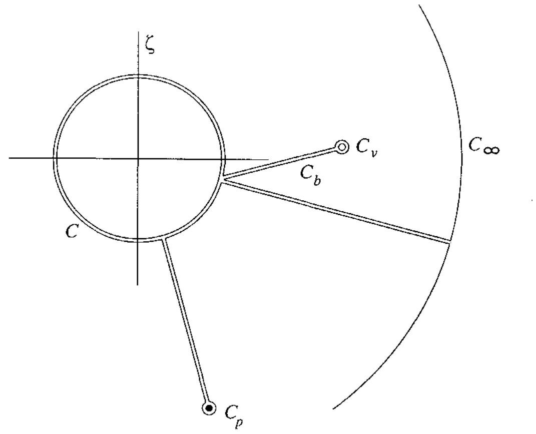

Fig. B1 Integration contour for moment.

$$\mathcal{C} = -\frac{r_c^2a^2}{\zeta_c^2} + \frac{r_c^2a^4}{\left(r_c^2-\delta^2\right)^2} \tag{B7}$$

$$\mathcal{D} = -\frac{r_c^2a^4}{\left(r_c^2-\delta^2\right)^2} \tag{B8}$$

$$\mathcal{E} = -\frac{r_c^2a^4}{\left(r_c^2-\delta^2\right)\bar\zeta_c} + \frac{r_c^2a^2\zeta_c}{\bar\zeta_c^2} \tag{B9}$$

$$\mathcal{F} = \frac{r_c^2a^2}{\bar\zeta_c^2} \tag{B10}$$

It is now apparent that g has a pole at $\zeta = -r_c^2/\bar\zeta_c$, in addition to the singularities inside C and at ζ_k. The integration contour in the ζ plane is shown in Fig. B1. The branch cut between the vortex and its image runs inside C_b, which intersects C at the point that maps onto the trailing edge, $\zeta = a - \zeta_c$; C_p surrounds the pole at $-r_c/\bar\zeta_c$, and the contour is closed at a large distance by C_∞. We have

$$\int_C = \int_{C_\infty} - \int_{C_p} - \int_{C_b} \tag{B11}$$

The vortex at ζ_k has a logarithmic singularity, which is too weak to give a contribution as C_v shrinks.

The terms of g that go like $1/\zeta$ in the far field are easily identified, and we get the following contribution from C_∞:

$$\int_{C_\infty} g(\zeta)\,\mathrm{d}\zeta = -2\pi(\mathcal{A}+\mathcal{C}+\mathcal{D}+\mathcal{F})\log\frac{-r_c}{\zeta_k} \tag{B12}$$

The contribution from C_p is found from the residue of a first- and second-order pole:

$$\int_{C_p} g(\zeta)\,\mathrm{d}\zeta = 2\pi i\left\{\mathcal{D}i\log\frac{-r_c(\zeta-\zeta_k)}{\zeta_k\left(\zeta-r_c^2/\bar\zeta_k\right)}\right.$$

$$\left.+\frac{\mathrm{d}}{\mathrm{d}\zeta}\left[(\mathcal{E}+\mathcal{F}\zeta)i\cdot\log\frac{-r_c(\zeta-\zeta_k)}{\zeta_k\left(\zeta-r_c^2/\bar\zeta_k\right)}\right]\right\}_{\zeta=-r_c^2/\bar\zeta_c}$$

$$= -2\pi\left[(\mathcal{D}+\mathcal{F})\log\frac{-r_c\left(r_c^2/\bar\zeta_c+\zeta_k\right)}{\zeta_k\left(r_c^2/\bar\zeta_c+r_c^2/\bar\zeta_k\right)}\right.$$

$$\left.+\left(\mathcal{E}-\mathcal{F}r_c^2/\bar\zeta_c\right)\cdot\left(-\frac{1}{r_c^2/\bar\zeta_c+\zeta_k} + \frac{1}{r_c^2/\bar\zeta_c+r_c^2/\bar\zeta_k}\right)\right] \tag{B13}$$

The contribution from C_b can be evaluated using the fact that the logarithmic term in $g(\zeta)$ makes a jump of 2π from the upper to the lower bank of C_b. Thus

$$\int_{C_b} g(\zeta)\,\mathrm{d}\zeta = \int_{a-\zeta_c}^{\zeta_k} 2\pi\left[\frac{\mathcal{A}}{\zeta} + \frac{\mathcal{B}}{\zeta^2} + \frac{\mathcal{C}}{\zeta+\zeta_c} + \frac{\mathcal{D}}{\zeta + r_c^2/\bar{\zeta}_c} + \frac{\mathcal{E}+\mathcal{F}\zeta}{\left(\zeta + r_c^2/\bar{\zeta}_c\right)^2}\right]\mathrm{d}\zeta \tag{B14}$$

This is a sum of elementary line integrals in ζ, running from $a-\zeta_c$ to ζ_k. The last term is conveniently evaluated by integrating by parts, and we have

$$\begin{aligned}\int_{C_b} g(\zeta)\,\mathrm{d}\zeta &= 2\pi\mathcal{A}\log\frac{\zeta_k}{a-\zeta_c} - 2\pi\mathcal{B}\left(\frac{1}{\zeta_k} - \frac{1}{a-\zeta_c}\right)\\ &+ 2\pi\mathcal{C}\log\frac{\zeta_c+\zeta_k}{a} + 2\pi(\mathcal{D}+\mathcal{F})\log\frac{r_c^2/\bar{\zeta}_c+\zeta_k}{a-\zeta_c+r_c^2/\bar{\zeta}_c}\\ &- 2\pi\frac{\mathcal{E}+\mathcal{F}\zeta_k}{\zeta_k + r_c^2/\bar{\zeta}_c} + 2\pi\frac{\mathcal{E}+\mathcal{F}(a-\zeta_c)}{a-\zeta_c+r_c^2/\bar{\zeta}_c}\end{aligned} \tag{B15}$$

Then, all of the terms can be collected to find

$$\begin{aligned} I_5 &= 2\pi\mathcal{A}\log\frac{\zeta_c - a}{r_c} + 2\pi\mathcal{B}\left(\frac{1}{\zeta_k} - \frac{1}{a-\zeta_c}\right)\\ &- 2\pi\mathcal{C}\log\frac{-r_c(\zeta_c+\zeta_k)}{a\zeta_k} + 2\pi\mathcal{D}\log\frac{a-\zeta_c+r_c^2/\bar{\zeta}_c}{r_c^2/\bar{\zeta}_c + r_c^2/\bar{\zeta}_k}\\ &+ 2\pi\mathcal{E}\left(\frac{1}{r_c^2/\bar{\zeta}_c + r_c^2/\bar{\zeta}_k} - \frac{1}{a-\zeta_c+r_c^2/\bar{\zeta}_c}\right)\\ &+ 2\pi\mathcal{F}\left(\log\frac{a-\zeta_c+r_c^2/\bar{\zeta}_c}{r_c^2/\bar{\zeta}_c + r_c^2/\bar{\zeta}_k} + 1 - \frac{\bar{\zeta}_k}{\bar{\zeta}_k+\bar{\zeta}_c}\right.\\ &\left. - \frac{a-\zeta_c}{a-\zeta_c+r_c^2/\bar{\zeta}_c}\right)\end{aligned} \tag{B16}$$

Upon taking the real part, the logarithmic terms cancel, as expected, because the logarithm is a multivalued function. Now, employing the relation

$$r_c^2 = (a-\zeta_c)(a-\bar{\zeta}_c) \tag{B17}$$

we get

$$\begin{aligned}\mathrm{Re}\left\{\int_S w_5 z\,\mathrm{d}\bar{z}\right\} &= 2\pi\,\mathrm{Re}\left\{\mathcal{B}\left(\frac{1}{\zeta_k} - \frac{1}{a-\zeta_c}\right)\right.\\ &\left.+ \mathcal{E}\left[\frac{1}{r_c^2/\bar{\zeta}_c + r_c^2/\bar{\zeta}_k} - \frac{\bar{\zeta}_c}{a(a-\zeta_c)}\right] + \mathcal{F}\left(\frac{\bar{\zeta}_c}{\bar{\zeta}_k+\bar{\zeta}_c} - \frac{\bar{\zeta}_c}{a}\right)\right\}\end{aligned} \tag{B18}$$

Individually, $\mathcal{B}$, $\mathcal{E}$, and $\mathcal{F}$ blow up for $\zeta_c = 0$, and so this expression is not suitable for the special case of a flat plate. With this in mind, we can substitute the expressions for $\mathcal{B}$, $\mathcal{E}$, and $\mathcal{F}$ and make the troublesome terms cancel each other to obtain Eq. (43).

Letting $\zeta_k \to \infty$ in the previous expression yields Eq. (42).

Acknowledgments

Financial support of the Advanced Research Projects Agency, the Office of Naval Research, under Contracts N00014-92-J-1726 and N00014-93-1-0587, and the Sea Grant Program under Grant NA90AA-D-SG424 is gratefully acknowledged.

References

[1]Basu, B. C., and Hancock, G. J., "The Unsteady Motion of a Two-Dimensional Aerofoil in Incompressible Inviscid flow," *Journal of Fluid Mechanics*, Vol. 87, July 1978, pp. 159–178.

[2]Giesing, J. P., "Nonlinear Two-Dimensional Unsteady Potential Flow with Lift," *Journal of Aircraft*, Vol. 5, No. 2, 1968, pp. 135–143.

[3]Mook, D. T., Roy, S., Choksi, G., and Dong, B., "Numerical Simulation of the Unsteady Wake Behind an Airfoil," *Journal of Aircraft*, Vol. 26, No. 6, 1989, pp. 509–514.

[4]Choi, D. H., and Landweber, L., "Inviscid Analysis of Two-Dimensional Airfoils in Unsteady Motion Using Conformal Mapping," *AIAA Journal*, Vol. 28, No. 12, 1990, pp. 2025–2033.

[5]Mook, D. T., and Dong, B., "Perspective: Numerical Simulations of Wakes and Blade-Vortex Interaction," *Journal of Fluids Engineering*, Vol. 116, No. 1, 1994, pp. 5–21.

[6]McCroskey, W. J., "Unsteady Airfoils," *Annual Review of Fluid Mechanics*, Vol. 14, 1982, pp. 285–311.

[7]Sarpkaya, T., "An Inviscid Model of Two-Dimensional Vortex Shedding for Transient and Asymptotically Steady Separated Flow over an Inclined Plate," *Journal of Fluid Mechanics*, Vol. 68, March 1975, pp. 109–128.

[8]Saffman, P. G., and Sheffield, J. S., "Flow over a Wing with an Attached Free Vortex," *Studies in Applied Mathematics*, Vol. 57, No. 2, 1977, pp. 107–117.

[9]Sheen, Q.-Y., "Potential Flow Analysis of Unsteady Joukowski Airfoil in the Presence of Discrete Vortices," Ph.D. Thesis, Dept. of Aerospace Engineering Sciences, Univ. of Colorado, Boulder, CO, 1986.

[10]Panaras, A. G., "Numerical Modeling of the Vortex/Airfoil Interaction," *AIAA Journal*, Vol. 25, No. 1, 1987, pp. 5–11.

[11]Dickinson, A. L., "Computation of the Forces and the Far-Field Sound Radiation from an Unsteady Two-Dimensional Airfoil Using the Vortex Method," M.S. Thesis, Dept. of Mechanical Engineering, Massachusetts Inst. of Technology, Cambridge, MA, 1988.

[12]Milne-Thomson, L. M., *Theoretical Hydrodynamics*, 4th ed., MacMillan, New York, 1960, Chaps. 5, 9, and 13.

[13]Batchelor, G. K., *An Introduction to Fluid Mechanics*, 1st paperback ed., Cambridge Univ. Press, New York, 1967, p. 417.

[14]Streitlien, K., "A Simulation Procedure for Vortex Flow over an Oscillating Wing," Massachusetts Inst. of Technology Sea Grant, Rept. MITSG 94-7, Cambridge, MA, 1994.

[15]Clements, R. R., "An Inviscid Model of Two-Dimensional Vortex Shedding," *Journal of Fluid Mechanics*, Vol. 57, 1973, pp. 321–336.

[16]Sarpkaya, T., "Computational Methods with Vortices—The 1988 Freeman Scholar Lecture," *Journal of Fluids Engineering*, Vol. 111, No. 1, 1989, pp. 5–52.

[17]Greengard, L., and Rokhlin, V., "A Fast Algorithm for Particle Simulations," *Journal of Computational Physics*, Vol. 73, Dec. 1987, pp. 325–348.

[18]Carrier, J., Greengard, L., and Rokhlin, V., "A Fast, Adaptive Multipole Algorithm for Particle Simulations," *SIAM Journal on Scientific and Statistical Computing*, Vol. 9, No. 4, 1988, pp. 669–686.

[19]Korsmeyer, F. T., "An Order N Algorithm for the Solution of the Boundary Integral Equations of Potential Flow," *Fifth International Workshop on Water Waves and Floating Bodies*, Univ. of Manchester, Manchester, England, UK, 1990, pp. 97–101.

[20]Graham, J. M. R., "The Forces on Sharp-Edged Cylinders in Oscillatory Flow at Low Keulegan-Carpenter Number," *Journal of Fluid Mechanics*, Vol. 97, March 1980, pp. 331–346.

[21]Newman, J. N., *Marine Hydrodynamics*, 1st ed., MIT Press, Cambridge, MA, 1977, pp. 139–140.

[22]Sedov, L. I., *Two-Dimensional Problems in Hydrodynamics and Aerodynamics*, 1st ed., Interscience, New York, 1965, pp. 20–30.

[23]Chow, C.-Y., and Huang, M.-K., "The Initial Lift and Drag of an Impulsively Started Airfoil of Finite Thickness," *Journal of Fluid Mechanics*, Vol. 118, May 1982, pp. 393–409.

[24]McCune, J. E., and Tavares, T. S., "Perspective: Unsteady Wing Theory—The Kármán/Sears Legacy," *Journal of Fluids Engineering*, Vol. 115, No. 4, 1993, pp. 548–560.